Monthly Notices
of the
ROYAL ASTRONOMICAL SOCIETY

MNRAS **494,** 915–922 (2020)
Advance Access publication 2020 March 18

doi:10.1093/mnras/staa747

The White Dwarf Binary Pathways Survey – III. Contamination from hierarchical triples containing a white dwarf

F. Lagos,[1,2,3★] M. R. Schreiber,[1,2★] S. G. Parsons,[4] A. Zurlo,[5] D. Mesa,[6] B. T. Gänsicke,[7,8] R. Brahm,[9,10,11] C. Caceres,[2,12] H. Canovas,[13] M-S. Hernandez,[1] A. Jordan,[10,14] D. Koester,[15] L. Schmidtobreick,[3] C. Tappert[1] and M. Zorotovic[1]

[1]*Instituto de Física y Astronomía, Universidad de Valparaíso, Valparaíso, Chile*
[2]*Millennium Nucleus for Planet Formation, NPF, Universidad de Valparaíso, Valparaíso, Chile*
[3]*Nucleo de Astronomia, Facultad de Ingenieria y Ciencias, Universidad Diego Portales, Av. Ejercito 441, Santiago, Chile*
[4]*Department of Physics, University of Warwick, Coventry CV4 7AL, UK*
[5]*Instituto de Astrofsica, Facultad de Fsica, Pontificia Universidad Catolica de Chile, Av. Vicuna Mackenna 4860, 7820436 Macul, Santiago, Chile*
[6]*Millennium Institute of Astrophysics,Santiago, Chile*
[7]*Departamento de Ciencias Fisicas, Facultad de Ciencias Exactas, Universidad Andres Bello, Av. Fernandez Concha 700, Las Condes, Santiago, Chile*
[8]*Aurora Technology B.V., ESA-ESAC, Camino Bajo del Castillo s/n, 28692 Villanueva de la Cañada, Madrid, Spain*
[9]*Institut für Theoretische Physik und Astrophysik, Universität Kiel, D-24098 Kiel, Germany*
[10]*European Southern Observatory (ESO), Alonso de Cordova 3107, Vitacura, Santiago, Chile*
[11]*INAF – Osservatorio Astronomico di Padova, Padova, Italy*
[12]*Center of Astro-Engineering UC, Pontificia Universidad Católica de Chile, Av. Vicuña Mackenna 4860, 7820436 Macul, Santiago, Chile*
[13]*Department of Physics and Astronomy, University of Sheffield, Sheffield S3 7RH, UK*
[14]*Centre for Exoplanets and Habitability, University of Warwick, Coventry CV4 7AL, UK*
[15]*Facultad de Ingeniera y Ciencias, Universidad Adolfo Ibanez, Santiago, Chile*

Accepted 2020 March 13. Received 2020 March 12; in original form 2020 March 5

ABSTRACT

The *White Dwarf Binary Pathways Survey* aims at increasing the number of known detached A, F, G, and K main-sequence stars in close orbits with white dwarf companions (WD+AFGK binaries) to refine our understanding about compact binary evolution and the nature of Supernova Ia progenitors. These close WD+AFGK binary stars are expected to form through common envelope evolution, in which tidal forces tend to circularize the orbit. However, some of the identified WD+AFGK binary candidates show eccentric orbits, indicating that these systems are either formed through a different mechanism or perhaps they are not close WD+AFGK binaries. We observed one of these eccentric WD+AFGK binaries with SPHERE and find that the system TYC 7218-934-1 is in fact a triple system where the WD is a distant companion. The inner binary likely consists of the G-type star plus an unseen low-mass companion in an eccentric orbit. Based on this finding, we estimate the fraction of triple systems that could contaminate the WD+AFGK sample. We find that less than 15 per cent of our targets with orbital periods shorter than 100 d might be hierarchical triples.

Key words: methods: numerical – methods: statistical – binaries: close – stars: kinematics and dynamics.

1 INTRODUCTION

The unique potential of Type Ia Supernovae (SN Ia) as distance indicators, sufficiently bright to serve as yardsticks on cosmological distance scales (Branch & Tammann 1992), has made them some of the most important objects for our understanding in the Universe and has led to the discovery of its accelerating expansion (Riess et al. 1998; Perlmutter et al. 1999). Despite its importance, it is not clear which evolutionary pathways lead to SN Ia explosions, and the SN Ia progenitor puzzle remains a crucial unsolved astronomical question.

The two main formation channels for SN Ia explosions, i.e. the single (Webbink 1984) and double (Iben & Tutukov 1984) degenerate channels, involve thermonuclear explosions of WDs close to the Chandrasekhar mass limit. However, in recent years it has become evident that reaching a mass close to the Chandrasekhar limit

★ E-mail: felipe.lagos@postgrado.uv.cl (FL); matthias.schreiber@uv.cl (MRS)

might not be a strict criterion for SN Ia explosions, enlarging the possible evolutionary scenarios towards single or double degenerate SN Ia detonations (Fink, Hillebrandt & Röpke 2007; Guillochon et al. 2010; Kromer et al. 2010; Sim et al. 2010; van Kerkwijk, Chang & Justham 2010; Pakmor et al. 2013; Brooks et al. 2016). The situation has become even more complex as recently suggested evolutionary channels such as the core-degenerate (Livio & Riess 2003; Soker 2013; Aznar-Siguán et al. 2015) and the WD collisional scenario (Raskin et al. 2009; Rosswog et al. 2009) represent possible alternatives to the classical single and double degenerate channels.

In spite of the growing variety of potential SN Ia progenitor systems, it is clear that the progenitors are close binaries that contain at least one WD. However, it remains an open question how these close binaries form and how frequently a given SN Ia progenitor configuration is produced. Usually the initial main-sequence binary, consisting of two stars with masses exceeding $1\,M_{\odot}$, is assumed to evolve through a common envelope phase (e.g. Webbink 1984; Zorotovic et al. 2010) to generate the small binary separations required for any interaction between the stars. The close binary emerging from the common envelope phase, i.e. the post-common envelope binary (PCEB), consists of a WD and a main-sequence companion star. The orbital separation of a recently formed PCEB largely determines the future evolution of the system. Broadly speaking, if the orbital period is longer than 1–2 d, a second phase of mass transfer will be initiated when the secondary star evolves off the main sequence which, depending on the mass ratio of the system, may lead to a second common envelope phase and potentially to a double degenerate binary. If the orbital periods are shorter than 1–2 d, angular momentum loss can drive the system into mass transfer when the secondary star is still on the main sequence, which, again depending on the mass ratio of the binary system, can cause thermally unstable mass transfer and stable nuclear burning on the surface of the WD. Such systems, called super soft X-ray sources, are considered possible single degenerate SN Ia progenitors (Parsons et al. 2015).

Current binary population models rely on simple equations for common envelope evolution and, unfortunately, the common envelope efficiency is only well constrained for low-mass companions (Zorotovic et al. 2010; Nebot Gómez-Morán et al. 2011) which are irrelevant for SN Ia progenitor studies. It is therefore currently impossible to use binary population models to reliably predict relative numbers of SN Ia explosions generated by the single or the double degenerate channels.

To progress with this situation, we began a large-scale survey of PCEBs, consisting of main-sequence stars of spectral type AFGK plus a WD. As the WD is outshined by the AFGK secondary stars at optical wavelengths, we combine spectroscopic surveys with the Galaxy Evolution Explorer (*GALEX*) data base to identify AFGK stars with UV excess indicative of a WD companion (Parsons et al. 2016; Rebassa-Mansergas et al. 2017). We then use radial velocity measurements to identify the close binary systems and to measure their periods. So far, we have identified the first pre-supersoft X-ray binary system (Parsons et al. 2015), confirmed that our target selection is reliable and contains few contaminants (Parsons et al. 2016), and have published the first results of our radial velocity campaign (Rebassa-Mansergas et al. 2017).

One of our close WD+AFGK candidate stars identified by matching data from *GALEX* and the radial velocity experiment (RAVE) survey (Parsons et al. 2016) was the G-star TYC 7218-934-1 (henceforth TYC 7218). We here present radial velocity measurements of this object and find a short orbital period of 13.6 d, with an unexpected high eccentricity of $e = 0.46$. This eccentricity excludes CE evolution for the origin of the current short period. Investigating the origin of the eccentric orbit using high-contrast imaging, we find that TYC 7218 is in fact a hierarchical triple star system with the WD being the tertiary component. We estimate that such triple star systems contaminate our PCEB sample by $\lesssim$15 per cent.

2 TYC 7218 AS A TARGET OF THE SN IA PATHWAY PROJECT

As described in detail in Parsons et al. (2016), we identify WD+AFGK candidate binaries using UV excesses found by cross-matching optical surveys with *GALEX* data. TYC 7218 was one of our *RAVE* targets where we found clear evidence for a UV excess in *GALEX*. We consequently followed up this object with high-resolution spectroscopy to determine the orbital period of the binary and to obtain more information on the properties of its stellar components.

2.1 Characterizing the G-type star

We obtained high-resolution spectroscopy of TYC 7218 with the echelle spectrograph (resolving power $R \simeq 40\,000$; wavelength range ~3700 to ~7000 Å) on the 2.5-m Du Pont telescope located at Las Campanas Observatory, Chile, and with FEROS ($R \sim 48\,000$; ~3500 to ~9200 Å) on the 2.2-m Telescope at La Silla, Chile. Data obtained with both of these spectrographs were extracted and analysed using the Collection of Elemental Routines for Echelle Spectra (CERES) package (Brahm, Jordán & Espinoza 2017), which was developed to process spectra coming from different instruments in an homogeneous and robust manner. After performing standard image reductions, spectra were optimally extracted following Marsh (1989) and calibrated in wavelength using reference ThAr Lamps. For FEROS data, the instrumental drift in wavelength through the night was corrected with a secondary fiber observing a ThAr lamp. In the case of the Du Pont data, ThAr spectra were acquired before and after each science observation. Wavelength solutions were shifted to the barycentre of the Solar system.

We estimated the stellar parameters for the main-sequence star in TYC 7218 by comparing the observed data against a synthetic grid of stellar spectra (Coelho et al. 2005). The synthetic spectra were degraded to the resolution of the Du Pont echelle and FEROS by convolving them with a Gaussian. The optimal fit for each spectrum was found by chi-square minimization. We then combined the results from each spectral fit and used the average values, yielding an effective temperature $T_{\rm eff} = 5790 \pm 50$ K, surface gravity $\log g = 4.51 \pm 0.05$ (in cgs units) and metallicity [Fe/H] $= 0.00 \pm 0.05$. Using the Torres relation (Torres, Andersen & Giménez 2010) we find a mass and radius of $1.04 \pm 0.02\,M_{\odot}$ and $1.06 \pm 0.06\,R_{\odot}$ for the G2V star in TYC 7218.

We also took a medium resolution spectrum ($R \sim 5000$) of TYC 7218 with X-shooter (D'Odorico et al. 2006) mounted at the Cassegrain focus of VLT-UT2 at Paranal on the 11th of May 2015. X-shooter is comprised of three detectors which permits to obtain simultaneous data from the UV cut-off at 0.3 μm to the K band at 2.4 μm. Our data consisted of three 60 s exposures, which were reduced using the standard pipeline release of the X-shooter common pipeline library (CPL) recipes (version 2.5.2). The instrumental response was removed and the spectrum flux calibrated by observing the spectrophotometric standard star LTT 3218. The spectrum was not corrected for telluric features. The X-shooter spectrum extends our spectroscopic coverage to shorter and longer

wavelengths and agrees well with the solution obtained from fitting our FEROS and Du Pont spectra.

2.2 The white dwarf component as seen with *HST*

The G-type star characterized in the previous section outshines the WD at optical wavelengths. As described in detail in Parsons et al. (2016), we spectroscopically observed nine UV-excess objects (WD+AFGK candidates) with *HST* in order to confirm that the excess is due to a WD companion. Depending upon the brightness of the target, we either used the Space Telescope Imaging Spectrograph (STIS) or the Cosmic Origins Spectrograph (COS). TYC 7218 was among our *HST* targets. We obtained two COS spectra of TYC 7218 on 2015 April 29 and May 7, each with an exposure time of 2175 s. We used the G130M grating centred on 1291 Å, resulting in a wavelength coverage 1130–1430 Å at a spectral resolution of ≃0.1 Å. We dithered the spectrum in the dispersion direction across all four FP-POS settings to mitigate fixed pattern noise of the COS detector. The data were reduced with CALCOS V3.1.1.

The broad Ly α line and the blue continuum confirm that the *UV* excess detected with *GALEX* is due to the presence of a hot compact object: a WD. In contrast to the close binary TYC 6760-497-1 (Parsons et al. 2015), no sharp metal lines were detected, hence it was not possible to measure the radial velocity of the WD.

Parsons et al. (2016) performed a preliminary analysis of the effective temperature of the WD in TYC 7218 and obtained $T_{\rm eff} \simeq 16\,500$ K, assuming a fixed WD mass of $M_{\rm WD} = 0.6\,{\rm M}_{\odot}$. To improve upon this estimate, we re-analysed the COS spectrum making use of the accurate distance to TYC 7218 provided by the *Gaia* Data Release 2 (DR2) parallax measurement (Gaia Collaboration 2018) and a grid of hydrogen model atmospheres spanning $T_{\rm eff} = 14\,000$–$40\,000$ K and surface gravities of $\log g = 7.5$–9.4 which were computed with the code of Koester (2010).

For a fixed $\log g$, a fit to the COS spectrum results in $T_{\rm eff}$, and using the cooling models of Holberg & Bergeron (2006), Kowalski & Saumon (2006), and Tremblay, Bergeron & Gianninas (2011),[1] we can calculate the mass and radius of the WD. The scaling factor between the model spectrum and the COS data relates to the WD radius ($R_{\rm WD}$) and distance as

$$\frac{F_{\rm COS}}{H_{\rm mod}} = 4\pi \frac{{R_{\rm WD}}^2}{d^2} \quad (1)$$

with $F_{\rm COS}$ the observed flux and $H_{\rm mod}$ the Eddington flux of the model. We then iterate the fit over $\log g$ until the distance implied by the fit agrees with that implied by the *Gaia* DR2 parallax, $d = 183.8 \pm 1.6$ pc. Fitting the two COS spectra individually, and assuming zero reddening, the best-fitting parameters obtained are $T_{\rm eff} = 17\,255 \pm 36$ K and $\log g = 8.222 \pm 0.015$ (2015 April 29) and $T_{\rm eff} = 17\,106 \pm 38$ K and $\log g = 8.179 \pm 0.016$ (2015 May 7). The given uncertainties are purely statistical in nature, and the discrepancy between the two fits indicates that additional systematic uncertainties dominate the results. We adopt $T_{\rm eff} = 17\,126 \pm 150$ K and $\log g = 8.19 \pm 0.03$ as the final parameters, obtained from fitting the combined COS spectra and estimating the total uncertainties from the fits to the individual COS observations. The WD mass implied by these atmospheric parameters is $M_{\rm WD} = 0.73 \pm 0.03\,{\rm M}_{\odot}$. Repeating the previous analysis, but considering a reddening $E(B-V) = 0.017$[2] in the spectral fit, does not lead to significant differences

[1] http://www.astro.umontreal.ca/~bergeron/CoolingModels/
[2] https://stilism.obspm.fr

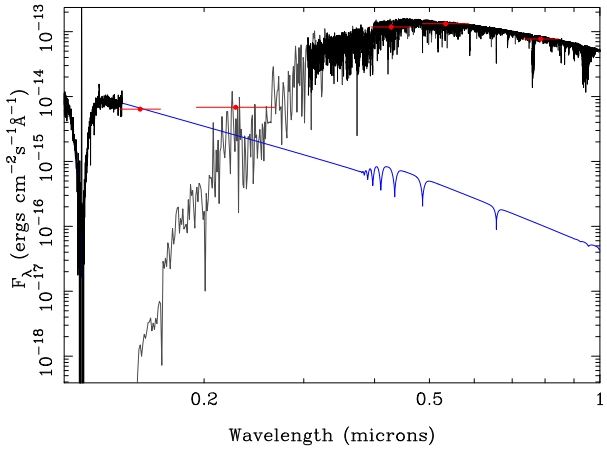

Figure 1. Spectral energy distribution of TYC 7218. The thick black lines show the X-shooter and the *HST* spectrum, while red dots correspond to photometric measurements. The best fit to the system is obtained with a G2V main-sequence star (thin black line) and a WD with an effective temperature of $T_{\rm eff} = 17\,126 \pm 150$ K (blue line).

(≈ 2 per cent) in the final parameters of the WD compared to the zero-reddening case. The *HST* and X-shooter spectra are shown in Fig. 1 together with the best fit for the WD and the G-type star.

2.3 The radial velocity curve of TYC 7218

The observing strategy of our SN Ia pathway project is to take a few spectra per object in our UV excess target sample to test for radial velocity variations. If radial velocity variations are detected, we then aim at measuring the orbital period of the close binary. The first two spectra taken of TYC 7218 with the Echelle spectrograph at the Du Pont telescope clearly showed small but significant radial velocity variations (see Table 1). We therefore followed up the system with the Du Pont/Echelle and MPG2.2/FEROS spectrographs until the orbital period was clearly measured.

The radial velocities were computed from the optical echelle spectra using the cross-correlation technique against a binary mask representative of a G2-type star. The uncertainties in radial velocity were computed using scaling relations (for more detail see Jordán et al. 2014) with the signal-to-noise ratio and width of the cross-correlation peak, which were calibrated with Monte Carlo simulations. The observing dates and the obtained radial velocities are shown in Table 1.

Based on the radial velocities we measured the orbital parameters of TYC 7218-934-1 using EXOFAST (Eastman, Gaudi & Agol 2013). The best-fitting orbit is shown in Fig. 2 and has a period of 13.6 d with an eccentricity of $e = 0.46$. The full orbital solution is detailed in Table 2. Using the binary mass function, the minimum mass of the companion to the G2V star is $0.2\,{\rm M}_{\odot}$.

The eccentric orbit of a binary star that contains a G-type star and a WD with an orbital period of just 13.6 d is puzzling. Such close WD binaries are supposed to form through common envelope evolution, in which drag forces within the envelope should quickly circularize the orbit. As this quick circularization is a rock-solid prediction of common envelope theories, the close eccentric binary in TYC 7218 must have either formed due to the action of another mechanism or the WD is not responsible for the velocity variations measured for the G2-type secondary star.

As a non-negligible fraction (≃ 40 per cent) of close main-sequence binary stars with orbital periods around 13 d are often

Table 1. Radial velocity measurements for the G star in TYC 7218-934-1.

BJD (TDB) (mid-exposure)	Velocity ($km\,s^{-1}$)	Uncertainty ($km\,s^{-1}$)	Telescope/ instrument
2456809.55612643	9.966	0.500	Du Pont/Echelle
2456810.53044180	6.760	0.500	Du Pont/Echelle
2456810.64079226	5.518	0.500	Du Pont/Echelle
2456811.46154176	1.996	0.500	Du Pont/Echelle
2456811.52899051	1.177	0.500	Du Pont/Echelle
2456811.63107790	0.078	0.500	Du Pont/Echelle
2456827.46756122	− 3.923	0.010	MPG2.2/FEROS
2456827.53633937	− 2.975	0.010	MPG2.2/FEROS
2456828.46953698	16.493	0.010	MPG2.2/FEROS
2456828.55232328	17.966	0.010	MPG2.2/FEROS
2456829.52614915	26.724	0.010	MPG2.2/FEROS
2456829.57929164	26.879	0.010	MPG2.2/FEROS
2456829.62074015	26.996	0.010	MPG2.2/FEROS
2456830.62692793	27.289	0.012	MPG2.2/FEROS
2456831.48604658	25.761	0.010	MPG2.2/FEROS
2456832.47118249	23.405	0.010	MPG2.2/FEROS
2456832.62146085	23.021	0.010	MPG2.2/FEROS
2456833.47375716	20.727	0.010	MPG2.2/FEROS
2456834.48096122	17.777	0.011	MPG2.2/FEROS
2456834.62990540	17.311	0.013	MPG2.2/FEROS
2456835.49422311	14.558	0.010	MPG2.2/FEROS
2456835.62537693	14.135	0.012	MPG2.2/FEROS
2457000.81838345	6.481	0.010	MPG2.2/FEROS
2457001.80957701	1.717	0.020	MPG2.2/FEROS
2457001.84002488	1.576	0.018	MPG2.2/FEROS
2457002.81549501	− 3.854	0.010	MPG2.2/FEROS
2457003.81567332	− 7.157	0.010	MPG2.2/FEROS
2457003.84959665	− 7.105	0.010	MPG2.2/FEROS
2457004.79505517	5.728	0.013	MPG2.2/FEROS
2457004.84905627	7.003	0.010	MPG2.2/FEROS
2457386.82926372	25.034	0.010	MPG2.2/FEROS

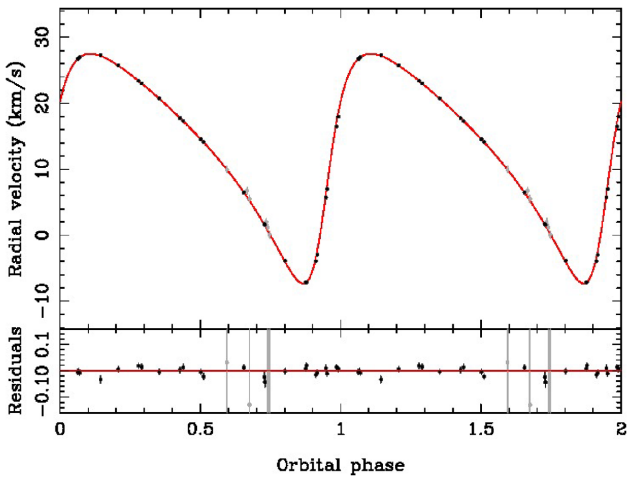

Figure 2. Phase-folded radial velocity plot for the main-sequence star in TYC 7218-934-1. The lower panel shows the residuals to the best fit. Data from the Du Pont echelle are shown in grey and from FEROS in black.

members of hierarchical triple systems (Tokovinin et al. 2006; Tokovinin 2014), such a configuration could represent a reasonable explanation for the eccentricity observed in TYC 7218. This hypothesis, however, leaves two quite distinct possibilities for the evolutionary history and current configuration of TYC 7218. First, it could indeed be a close WD+AFGK star with an unseen low-mass companion, where the close inner binary configuration was achieved through the Kozai–Lidov (KL) effect generated or enhanced by the mass-loss when the progenitor of the WD evolved off the main sequence (Shappee & Thompson 2013), or it might be a close main sequence star binary consisting of the G2V star and an unseen low-mass companion where the WD is the distant third object and not part of the inner binary star. In the latter case, the close inner main sequence binary star might have been affected by triple-system dynamics.

Table 2. Orbital parameters for TYC 7218-934-1. Parameters highlighted with a * were calculated assuming the G star has a mass of $1.04 \pm 0.02\,M_{\odot}$.

Parameter	Value	Error	Unit
Period	13.601 486	0.000 050	Days
Eccentricity	0.455	0.005	–
Argument of periastron	− 113.93	0.67	Degrees
Time of periastron	2456 895.867 56	0.000 03	BJD(TDB)
RV semi-amplitude	17.397	0.037	$km\,s^{-1}$
Systemic velocity	13.385	0.010	$km\,s^{-1}$
Semimajor axis*	0.113	0.001	au
Min. companion mass*	0.200	0.005	$M_{\odot}$

3 THE TRIPLE NATURE OF TYC 7218 CONFIRMED WITH SPHERE

To test the idea of TYC 7218 being a triple system, we observed it with the high contrast imager SPHERE (Beuzit et al. 2019) in the IRDIFS mode. Acquisition of direct imaging was made with IRDIS (Dohlen et al. 2008) in the dual band imaging mode (Vigan et al. 2010) using the *H*2–*H*3 bands with simultaneous spectro-imaging using IFS (Claudi et al. 2008) in the *Y* and *J* spectral bands. The aim of these observations was to confirm the triple nature of the system and to characterize the third object, i.e. to answer the question of whether it is a low-mass main-sequence star or the WD.

3.1 Data reduction

The SPHERE data were reduced exploiting the data reduction and handling (DRH – Pavlov, Feldt & Henning 2008) pipeline. The IRDIS data were first pre-processed (sky background subtraction, flat-fielding, and bad-pixels correction). The frames were recentred using the initial star centre exposure with the four satellite spots. The IFS pre-processing consists of background subtraction and flat-field calibration. Then, each frame was calibrated with the integral field unit (IFU) flat. For wavelength calibration, the IFU was illuminated with four monochromatic lasers of known wavelength. The result of this data pre-processing was a data cube of 39 monochromatic frames.

After pre-processing, IRDIS and IFS data were reduced with ad hoc IDL routines presented in Zurlo et al. (2014, 2016) to perform the angular differential imaging (ADI; Marois et al. 2006). The two IRDIS filters were processed with the KLIP (Soummer, Pueyo & Larkin 2012) method, as described in detail in Zurlo et al. (2016). The IFS data were processed using two independent codes that imply KLIP and a custom principal component analysis (PCA) code, as presented in Zurlo et al. (2016) and Mesa et al. (2015), respectively.

For the extraction of the spectrum, we used ADI separately for each individual IFS channel, since the object is very bright. We applied the fake negative planets technique (see e.g. Lagrange et al.

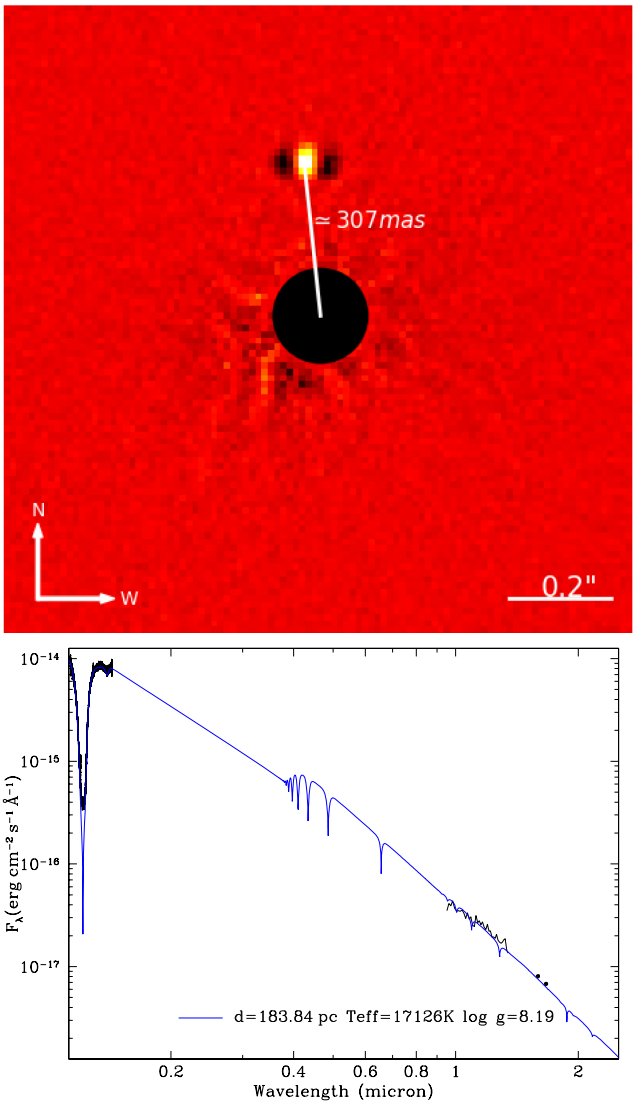

Figure 3. Upper panel: IRDIS image of the third object in the *H*2 band. The black circle denotes the position of the ALC_YJH_S coronograph. The projected separation of the WD relative to the central binary is 307 mas. Bottom panel: Spectral fit for the *HST* (black data at ≈1100 Å) and SPHERE data (black line at ≈10 000 Å) of TYC 7218. The blue line is the best fit for both *HST* and SPHERE data at 184 pc, the distance estimated by the GAIA DR2. The two black points, from left to right, are the *H*2 and *H*3 fluxes of the WD, respectively, with magnitude differences $\Delta H2 = 8.22 \pm 0.03$ and $\Delta H3 = 8.30 \pm 0.03$ with respect to the central binary.

2010; Bonnefoy et al. 2011), which is very effective in taking into account the self-subtraction of the flux.

3.2 A distant WD companion to a close main-sequence binary

The SPHERE IFS spectrum (which covers a wavelength range of 9000–10 400 Å) and the *H*2 (15 930 Å) and *H*3 (16 670 Å) fluxes are shown in Fig. 3, along with the COS spectrum of the system, and the best-fitting WD model to the COS data (Section 2.2). It is evident that the SPHERE observations are entirely consistent with the wide companion in TYC 7218 being the WD, located at an angular distance of 307 mas, rather than a low-mass K/M-type star. For completeness, we fitted the COS and SPHERE data together following the same procedure as in Section 2.2, and find $T_{\rm eff} = 17060 \pm 150$ K and $\log g = 8.17 \pm 0.02$, i.e. in agreement with the fit to the far-ultraviolet data alone.

To further support our interpretation of the SPHERE detection, we calculate the probability P(Θ, *m*) of chance alignments with background sources within an angular distance Θ. Following Brandner et al. (2000), we estimate this probability as

$$P(\Theta, m_{\rm lim}) = 1 - e^{-\pi\Theta\rho(m_{\rm lim})}, \quad (2)$$

where $\rho(m)$ is the cumulative surface density of background sources down to a limiting magnitude $m_{\rm lim}$. In order to calculate $\rho(m_{\rm lim})$, we use the Besançon galaxy model[3] (Czekaj et al. 2014) to generate a synthetic $JHK_{\rm s}$ photometric catalogue of point sources within 0.5 square degrees, centred in the coordinates of TYC 7218. The magnitude of the companion is $m_{\rm lim} \simeq 18.4$ in the *H* band, which results in a very low probability of $P(\Theta, m_{\rm lim}) = 10^{-4}$ for a background source to be located within $\Theta = 307$ mas of TYC 7218. We hence conclude that the SPHERE data unambiguously demonstrate that the wide component in the stellar triple TYC 7218 is a $\simeq 0.7\,{\rm M}_{\odot}$ WD.

This implies that the eccentric orbit of the G-type star most likely corresponds to an inner main-sequence binary with an unseen companion with a minimum stellar mass of $0.2\,{\rm M}_{\odot}$(as determined previously from the orbital solution, see Section 2.3). Assuming that the unseen companion is a main-sequence star, we constrain its maximum mass by testing up to which stellar mass we obtain agreement with the archival photometry of TYC 7218 in the *G*, *V*, *H*, *J*, and $K_{\rm s}$ bands. We used VOSA (Bayo et al. 2008) with the Koester (2010) and BT-settl spectra libraries for the WD and the main-sequence stars in the inner binary, respectively. For the unseen companion spectrum we used templates with $\log g = 5.0$, [Fe/H] = 0.0, and effective temperature spanning $T_{\rm eff} = 2500$–5800 K with a step size of $\Delta T_{\rm eff} = 500$ K. In total agreement with our interpretation of TYC 7218, the infrared photometry of the system fits better by including an additional component from the companion that is not seen in the optical spectra. We find acceptable fits (*p*-value < 0.05) for stellar temperatures from 3000 to 5000 K corresponding to stellar masses of 0.31–$0.80\,{\rm M}_{\odot}$ according to the Torres relation (Torres et al. 2010). The best-fitting model is obtained assuming a K-type star with $T_{\rm eff} = 4000$ K and mass of $0.55\,{\rm M}_{\odot}$.

4 THE POTENTIAL EVOLUTIONARY HISTORY OF THE TRIPLE SYSTEM

We confirmed the triple nature of TYC 7218, identifying the WD as the third object at a projected separation of ≈56 au (assuming a distance to the system of 184 pc) from the inner binary. This inner binary most likely consists of the G2V star and an (in the optical) unseen K–M dwarf main-sequence companion.

In order to investigate the possible evolutionary history of this triple system, we estimated whether it is likely that the observed inner eccentric orbit in TYC 7218 was caused by Kozai–Lidov mechanisms (KLMs), as close binaries with short orbital periods likely have tertiary companions (Tokovinin et al. 2006). To evaluate the current presence of eccentricity oscillations in the system due to the standard and eccentric KLMs (Lithwick & Naoz 2011) we compare their time-scales with the time-scale of general relativity precession, which can detune the eccentricity oscillations produced by the KLMs. According to Li et al. (2015), the time-scales of the

[3] https://model.obs-besancon.fr/modele_home.php

Table 3. Current parameters for TYC 7218-934-1. The outer orbit is only constrained by the projected separation of the tertiary detected with SPHERE. For the mass of the companion to the G star in the inner binary we can only derive a lower limit.

Parameter	Value	Unit
G star mass	1.04 ± 0.02	$M_\odot$
Companion mass	$0.2 \lesssim M \lesssim 0.8$	$M_\odot$
WD mass	0.73 ± 0.03	$M_\odot$
Inner period	$13.601\,486 \pm 0.000\,05$	d
Outer projected separation	56	au
Outer period	$\gtrsim 10^{4.8}$	d
Eccentricity	0.455 ± 0.005	–

standard KLM, eccentric KLM, and general relativity precession are

$$t_{\rm SKLM} = \frac{2\pi a_{\rm out}^3 \left(1-e_{\rm out}^2\right)^{3/2} \sqrt{(M_1+M_2)\left(1-e_{\rm in}^2\right)}}{G^{1/2} a_{\rm in}^{3/2} M_3}, \quad (3)$$

$$t_{\rm EKLM} = \frac{t_{\rm SKM}}{\epsilon_{\rm oct}} \quad (4)$$

and

$$t_{\rm GRP} = 2\pi \frac{a_{\rm in}^{5/2} c^2 \left(1-e_1^2\right)}{3G^{3/2}(M_1+M_2)^{3/2}}, \quad (5)$$

respectively, where a is the semimajor axis, e the eccentricity, M_1 and M_2 the masses of the stars in the inner binary and M_3 the mass of the third star, while the subscripts *in* and *out* refer to the inner and outer orbit. The term

$$\epsilon_{\rm oct} = \left|\frac{M_1-M_2}{M_1+M_2}\right| \left(\frac{a_{\rm in}}{a_{\rm out}}\right) \frac{e_{\rm out}}{1-e_{\rm out}^2} \quad (6)$$

measures the impact of the eccentric KLM on the orbital evolution of the system relative to the standard KLM. For $\epsilon_{\rm oct} \gtrsim 0.01$, the eccentricity oscillations due to the eccentric KLM become important (Lithwick & Naoz 2011). Thus, if $t_{\rm SKM} > t_{\rm GRP}$ or $t_{\rm EKM} > t_{\rm GRP}$ KL oscillations are suppressed by general relativity precession. To evaluate numerically equations (3)–(6), we assumed the projected separation we derived from the SPHERE observations to be the real separation of the third object at apastron, which represents a lower limit of the true value of $a_{\rm out}$. As the time-scale of KL oscillations decreases with the separation of the third star, this implies that, if in this assumed configuration KLMs are not important, they are clearly not important in TYC 7218 right now. As the eccentricity of the orbit of the third object is unknown, we leave it as a free parameter.

Using the system parameters summarized in Table 3, we find that KLMs could only be important for very high eccentricities of the outer orbit, exceeding ≈0.93 (see upper panel of Fig. 4). However, such high eccentricities would bring the system very close to being unstable despite the rather large difference in separation between the two orbits, as shown in the bottom panel of Fig. 4. We therefore conclude that it is very unlikely that the system is currently affected by KLMs. However, the fact that KLMs are currently not important does not imply that the evolution of the system was always unaffected by this mechanism. If KLMs plus tidal forces affected the inner orbit, it could have been much larger in the past, i.e. the current period (13.6 d) represents only a lower limit on the initial inner orbital period. Reconstructing the exact history of TYC 7218 is of course impossible, as the outer orbit is poorly constrained. However, the parameters we derived for TYC 7218 fit well into a

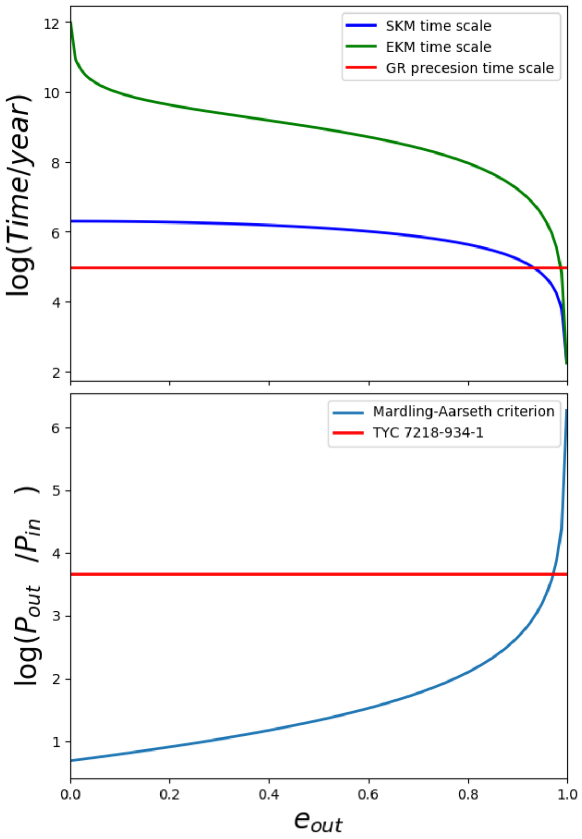

Figure 4. Upper panel: Comparison between the KL mechanisms time-scales (blue and green lines) and the general relativity precession time-scale (red line) for the TYC 7218 configuration given in Table 3, leaving the outer eccentricity $e_{\rm out}$ as a free parameter. Only for values of $e_{\rm out}$ greater than ≈0.93 and ≈0.98, the standard and eccentric KL oscillations are present. Bottom panel: Using the stability criterion derived by Mardling & Aarseth (2001) for the maximum ratio between inner and outer period (blue line), the highest eccentricity allowed for TYC 7218, given its current minimum period ratio (red line), is ≈0.97.

scenario for triple evolution recently suggested by Moe & Kratter (2018).

These authors propose that two different regimes exist for tidal effects in binary stars. For large eccentricities, strong dynamical tides dominate while for smaller eccentricities only weak tidal forces are expected. The eccentricity at which the transition between these two regimes occurs, the so-called transition eccentricity $e_{\rm trans}$, has been considered as a free parameter by Moe & Kratter (2018). However, they showed that setting $e_{\rm trans} = 0.5$ would explain the observed population of main-sequence triple systems with inner periods of less than 6 d. Interestingly, in the context of TYC 7218, according to this scenario, inner binaries should concentrate close to $e_{\rm trans}$ when the orbital period is above the circularization period which is $P_{\rm circ} = 11$ d for solar-type MS binaries (Raghavan et al. 2010). Therefore, with its inner eccentricity of 0.46 and its inner period of 13.6 d, TYC 7218 agrees very well with the scenario outlined by Moe & Kratter (2018).

Thus, a plausible scenario for the evolution of TYC 7218 can be described as follows: the initial configuration consisted of an inner binary with $P_{\rm in,0} > 100$ d affected by KL oscillations. The large eccentricities generated led to strong dynamical tides decreasing the orbital period and eccentricity of the inner binary. When the eccentricity became smaller than $e_{\rm trans} = 0.5$, the inner eccentricity

began to only very slowly decrease since weak-friction equilibrium-tide evolution is a slow process. When the eccentricity was close to its current value (0.455), the tertiary evolved into the WD we observe today. The corresponding mass-loss increased the outer period and turned off KLMs. In the future, the inner binary will continue to slowly circularize.

5 HOW MANY TRIPLES DO WE EXPECT TO HIDE AMONG THE WD/AFGK TARGETS?

As TYC 7218 has been identified in our survey of post common envelope binaries (PCEBs) consisting of WD+AFGK binaries, an urgent question is of course, how many more triples with a K–M dwarf and a WD, being each one either the tertiary component or the AFGK companion, might contaminate our sample. To roughly evaluate the possible contamination due to triple systems containing a WD and a K–M dwarf, we used the algorithm presented by Tokovinin (2014) and generated a population of binary and triple systems composed of zero-age main-sequence stars. As the algorithm only returns orbital periods and mass ratios, parameters like the eccentricities and inclination between the inner and outer orbits are assumed to follow the distributions used in Fabrycky & Tremaine (2007). Once the initial population is generated, we assign a born-time to each system from a uniform distribution between 0 and 10 Gyr, and select only those where one star (the most massive one of the system) had enough time to evolve into a WD. We then use the *Binary Stellar Evolution* (BSE) code (Hurley, Tout & Pols 2002) to evolve those systems that enter a common envelope phase when the more massive star of the binary (or the inner binary of a triple) evolves off the main sequence. For triples in which the most massive star evolves into a WD without interacting with the other stars in the system, we simply use the adiabatic mass-loss model to determine the effect on the orbital separations.

Based on this generated population of PCEBs and triples with configurations AFGK/WD+KM (the WD as part of the inner binary) and AFGK/KM+WD (the WD being the tertiary), we derive the upper and lower limit of the fraction of the triple system contamination. First, we obtain a lower limit on the fraction of triples in our sample by comparing the pure number of PCEBs (with AFGK secondary stars) with the number of triple systems with a WD tertiary (AFGK/KM+WD configuration) and with the inner binary having an orbital period shorter than 100 d, ignoring any possible triple dynamics. We find that PCEBs are roughly a hundred times more frequent than triples with white dwarfs tertiares. This value could be slightly higher ($\sim$2 per cent) as the simulator of Tokovinin (2014) does not fully reproduce the fraction of inner sub-systems with periods less than 100 d. In order to complement this lower limit with an upper limit, we derived the number of systems with an initial inner period longer than 100 d that are affected by KLMs either before or after the evolution of the most massive star into a WD. We find that the fraction of contaminants due to triple systems with configurations AFGK/WD+KM and AFGK/KM+WD increases to 15 per cent. We thus conclude that the contamination by triple systems of our sample is most likely in the range of 1–15 per cent.

To estimate this upper and lower limit we used the algorithm of Tokovinin (2014) and the distributions in Fabrycky & Tremaine (2007), which have been derived from observations of field stars with masses in the range $0.8 \lesssim M \lesssim 1.3\,\mathrm{M}_{\odot}$. This represents a reasonable approach although it contains rather rough approximations. First, we used these distributions to create a population of zero-age main-sequence binary and triple systems while they have been derived from observations of field stars. Triple stars in the field, however, may already be affected by evolutionary effects. These evolutionary effects might have led to a reduction of the inner period due to tidal effects which somewhat softens our lower limit. Secondly, we used the distributions for stellar components beyond the mass range of the observed sample. This approach should be correct in terms of the mass ratio and period distributions as those of intermediate and high-mass stars do not differ significantly from those used for sun-like stars (Duchêne & Kraus 2013). The multiplicity fractions, however, may significantly increase as a function of primary star mass. For example, nearly all B type stars seem to be members of multiple systems, with a triple fraction of $\sim$50 per cent (Toonen, Hamers & Zwart 2016; Moe & Kratter 2018). These larger multiplicity fractions for massive progenitor systems might somewhat soften our upper limit.

6 SUMMARY AND CONCLUSIONS

We report the discovery of the first hierarchical triple system in the *White Dwarf Binary Pathways Survey*. TYC 7218-934-1, initially identified as a G-type star orbited by a WD with a period of $P_{\rm in}$ =13.6 d, showed an eccentric orbit, being inconsistent with the circularization process of binaries that passed through the common envelope phase. Based on the hypothesis that the object is therefore rather a triple system than a post common envelope binary we observed TYC 7218 with the VLT/SPHERE in the IRDIFS mode to look for the third star. The performed observations confirmed the presence of a third object at a projected separation of $\approx$56 au from the inner binary, and the IFS spectrum in the *YJ*-band confirmed that this tertiary corresponds to the WD. We then performed binary and triple population synthesis to estimate the fraction of triple systems such as TYC 7218 that contaminate our sample of post common envelope WD+AFGK binaries. We found that $\approx$1–15 per cent of the observed close WD+AFGK binaries could be triple systems with a WD tertiary. This fraction of contaminating triple systems is clearly acceptable and therefore the project remains a promising pathway towards progressing with the SN Ia progenitor puzzle.

ACKNOWLEDGEMENTS

MRS acknowledges financial support from FONDECYT (grant number 1181404). SGP acknowledges the support of the STFC Ernest Rutherford Fellowship. AZ acknowledges support from the CONICYT/PAI (grant PAI77170087). BTG was supported by the UK STFC grant ST/P000495. RB acknowledges support from FONDECYT Post-doctoral Fellowship Project 3180246, and from the Millennium. Institute of Astrophysics (MAS). CC acknowledges support from DGI-UNAB project DI-11-19/R. MSH thanks Doctorado Nacional CONICYT 2017 folio 21170070. CT acknowledges financial support from Fondecyt No. 1170566. MZ acknowledges support from CONICYT/PAI (grant 79170121) and CONICYT/FONDECYT (grant 11170559). We also thank the referee Steve B. Howell for helpful suggestions that improved the presentation of this paper.

REFERENCES

Aznar-Siguán G., García-Berro E., Lorén-Aguilar P., Soker N., Kashi A., 2015, MNRAS, 450, 2948
Bayo A., Rodrigo C., Barrado Y Navascués D., Solano E., Gutiérrez R., Morales-Calderón M., Allard F., 2008, A&A, 492, 277
Beuzit J.-L. et al., 2019, A&A, 631, A155
Bonnefoy M. et al., 2011, A&A, 528, L15

Brahm R., Jordán A., Espinoza N., 2017, PASP, 129, 034002
Branch D., Tammann G. A., 1992, ARA&A, 30, 359
Brandner W. et al., 2000, AJ, 120, 950
Brooks J., Bildsten L., Schwab J., Paxton B., 2016, ApJ, 821, 28
Claudi R. U. et al., 2008, SPHERE IFS: The Spectro Differential Imager of the VLT for Exoplanets Search, SPIE, Marseille, France, p. 70143E
Coelho P., Barbuy B., Meléndez J., Schiavon R. P., Castilho B. V., 2005, A&A, 443, 735
Czekaj M. A., Robin A. C., Figueras F., Luri X., Haywood M., 2014, A&A, 564, A102
D'Odorico S. et al., 2006, in McLean I. S., Iye M., eds, Proc. SPIE Conf. Ser. Vol. 6269, Ground-based and Airborne Instrumentation for Astronomy. SPIE, Bellingham, p. 626933
Dohlen K. et al., 2008, The Infra-red Dual Imaging and Spectrograph for SPHERE: Design and Performance, SPIE, Marseille, France, p. 70143L
Duchêne G., Kraus A., 2013, ARA&A, 51, 269
Eastman J., Gaudi B. S., Agol E., 2013, PASP, 125, 83
Fabrycky D., Tremaine S., 2007, ApJ, 669, 1298
Fink M., Hillebrandt W., Röpke F. K., 2007, A&A, 476, 1133
Gaia Collaboration, 2018, A&A, 616, A1
Guillochon J., Dan M., Ramirez-Ruiz E., Rosswog S., 2010, ApJ, 709, L64
Holberg J. B., Bergeron P., 2006, AJ, 132, 1221
Hurley J. R., Tout C. A., Pols O. R., 2002, MNRAS, 329, 897
Iben I., Jr., Tutukov A. V., 1984, An Essay on Possible Precursors of Type-I Supernovae, vol. 109, Springer, p. 181
Jordán A. et al., 2014, ApJ, 148, 29
Koester D., 2010, Mem. Soc. Astron. Ital., 81, 921
Kowalski P. M., Saumon D., 2006, ApJ, 651, L137
Kromer M., Sim S. A., Fink M., Röpke F. K., Seitenzahl I. R., Hillebrandt W., 2010, ApJ, 719, 1067
Lagrange A.-M. et al., 2010, Science, 329, 57
Li G., Naoz S., Kocsis B., Loeb A., 2015, MNRAS, 451, 1341
Lithwick Y., Naoz S., 2011, ApJ, 742, 94
Livio M., Riess A. G., 2003, ApJ, 594, L93
Mardling R. A., Aarseth S. J., 2001, MNRAS, 321, 398
Marois C., Lafrenière D., Doyon R., Macintosh B., Nadeau D., 2006, ApJ, 641, 556
Marsh T. R., 1989, Publ. Astrono. Soc. Pac., 101, 1032
Mesa D. et al., 2015, A&A, 576, A121
Moe M., Kratter K. M., 2018, ApJ, 854, 44
Nebot Gómez-Morán A. et al., 2011, A&A, 536, A43
Pakmor R., Kromer M., Taubenberger S., Springel V., 2013, ApJ, 770, L8
Parsons S. G. et al., 2015, MNRAS, 452, 1754
Parsons S. G., Rebassa-Mansergas A., Schreiber M. R., Gänsicke B. T., Zorotovic M., Ren J. J., 2016, MNRAS, 463, 2125
Pavlov A., Feldt M., Henning T., 2008, Data Reduction and Handling for SPHERE, ASP, London, United Kingdom, p. 581
Perlmutter S. et al., 1999, ApJ, 517, 565
Raghavan D. et al., 2010, ApJS, 190, 1
Raskin C., Timmes F. X., Scannapieco E., Diehl S., Fryer C., 2009, MNRAS, 399, L156
Rebassa-Mansergas A. et al., 2017, MNRAS, 472, 4193
Riess A. G. et al., 1998, AJ, 116, 1009
Rosswog S., Kasen D., Guillochon J., Ramirez-Ruiz E., 2009, ApJ, 705, L128
Shappee B. J., Thompson T. A., 2013, ApJ, 766, 64
Sim S. A., Röpke F. K., Hillebrandt W., Kromer M., Pakmor R., Fink M., Ruiter A. J., Seitenzahl I. R., 2010, ApJ, 714, L52
Soker N., 2013, in Di Stefano R., Orio M., Moe M., eds, Proc. IAU Symp. 281, Binary Paths to Type Ia Supernovae Explosions. Kluwer, Dordrecht, p. 72
Soummer R., Pueyo L., Larkin J., 2012, ApJ, 755, L28
Tokovinin A., 2014, AJ, 147, 87
Tokovinin A., Thomas S., Sterzik M., Udry S., 2006, A&A, 450, 681
Toonen S., Hamers A., Zwart S. P., 2016, The Evolution of Hierarchical Triple Star-systems, Springer, Berlin, p. 36
Torres G., Andersen J., Giménez A., 2010, A&AR, 18, 67
Tremblay P.-E., Bergeron P., Gianninas A., 2011, ApJ, 730, 128
van Kerkwijk M. H., Chang P., Justham S., 2010, ApJ, 722, L157
Vigan A., Moutou C., Langlois M., Allard F., Boccaletti A., Carbillet M., Mouillet D., Smith I., 2010, Proc. of the conf. In the Spirit of Lyot 2010, Paris, France, p. E48
Webbink R. F., 1984, ApJ, 277, 355
Zorotovic M., Schreiber M. R., Gänsicke B. T., Nebot Gómez-Morán A., 2010, A&A, 520, A86
Zurlo A. et al., 2014, A&A, 572, A85
Zurlo A. et al., 2016, A&A, 587, A57

This paper has been typeset from a TEX/LATEX file prepared by the author.